

RESEARCH ARTICLE | MAY 16 2023

Random telegraph fluctuations in granular microwave resonators

Special Collection: [Electronic Noise: From Advanced Materials to Quantum Technologies](#)

M. Kristen ; J. N. Voss; M. Wildermuth ; H. Rotzinger  ; A. V. Ustinov 

 Check for updates

Appl. Phys. Lett. 122, 202602 (2023)

<https://doi.org/10.1063/5.0147430>


View
Online

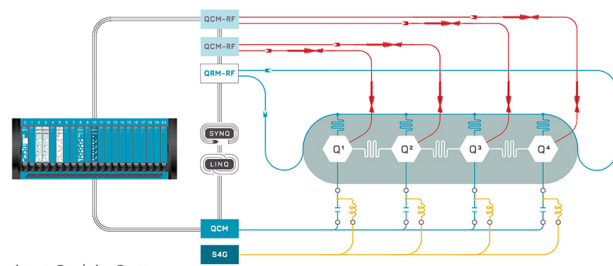

Export
Citation

CrossMark

 QBLOX

Integrates all
Instrumentation + Software
for Control and Readout of

Superconducting Qubits
NV-Centers
Spin Qubits



Superconducting Qubit Setup

[find out more >](#)

Random telegraph fluctuations in granular microwave resonators

Cite as: Appl. Phys. Lett. **122**, 202602 (2023); doi: [10.1063/5.0147430](https://doi.org/10.1063/5.0147430)

Submitted: 22 February 2023 · Accepted: 27 April 2023 ·

Published Online: 16 May 2023



View Online



Export Citation



CrossMark

M. Kristen,^{1,2}  J. N. Voss,² M. Wildermuth,²  H. Rotzinger,^{1,2,a)}  and A. V. Ustinov^{1,2} 

AFFILIATIONS

¹Institute for Quantum Materials and Technology, Karlsruhe Institute of Technology, 76344 Eggenstein-Leopoldshafen, Germany

²Physikalisches Institut, Karlsruhe Institute of Technology, 76131 Karlsruhe, Germany

Note: This paper is part of the APL Special Collection on Electronic Noise: From Advanced Materials to Quantum Technologies.

a) Author to whom correspondence should be addressed: rotzinger@kit.edu

ABSTRACT

Microwave circuit electrodynamics of disordered superconductors is a very active research topic spawning a wide range of experiments and applications. For compact superconducting circuit elements, the transition to an insulating state poses a limit to the maximum attainable kinetic inductance. It is, therefore, vital to study the fundamental noise properties of thin films close to this transition, particularly in situations where a good coherence and temporal stability is required. In this paper, we present measurements on superconducting granular aluminum microwave resonators with high normal state resistances, where the influence of the superconductor to insulator phase transition is visible. We trace fluctuations of the fundamental resonance frequency and observe, in addition to a $1/f$ noise pattern, a distinct excess noise, reminiscent of a random telegraph signal. The excess noise shows a strong dependency on the resistivity of the films as well as the sample temperature but not on the applied microwave power.

© 2023 Author(s). All article content, except where otherwise noted, is licensed under a Creative Commons Attribution (CC BY) license (<http://creativecommons.org/licenses/by/4.0/>). <https://doi.org/10.1063/5.0147430>

The phase transition from a superconducting to an insulating state (SIT) of disordered thin films remains under intense debate.^{1,2} The prevailing interest in the various aspects of this transition is owed to the intrinsic disorder of high- T_c superconductors^{3–5} as well as the use of disordered superconductors in quantum circuits and particle detectors.^{6–8}

Generally, the breakdown of the superconducting state manifests itself in the suppression of the long-range order parameter $\Psi = \Delta e^{i\phi}$. In the case of granular systems,⁹ it is believed that, while the amplitude Δ persists, the stiffness¹⁰ of the phase ϕ is lost when the effective Coulomb energy surpasses the energy of the Josephson coupling $E_J \propto \Delta/R_n$ between neighboring grains.^{11–13} This means that Cooper pairs, the charge carriers of the superconducting state, can no longer tunnel coherently between grains and the superconducting behavior of the whole sample is suppressed.^{14,15} In agreement with theoretical predictions,¹⁶ experiments have shown that this coincides with a normal state sheet resistance R_n on the order of the superconducting resistance quantum $R_q = 6.45 \text{ k}\Omega$.¹⁷

Disordered films in the vicinity of the SIT show a variety of intriguing physical effects, such as charge localization or subgap absorption. Experimental means to study such phenomena include

scanning tunneling microscopy (STM),^{18–22} optical spectroscopy,^{10,23–25} or transport measurements.^{26–29} While these techniques offer unique insight into the rich SIT physics, they provide only limited information regarding the applicability of these materials in high impedance microwave circuits, where they are sought after due to their sizable kinetic inductance $L_k \propto R_n$.

In this work, we attempt to bridge this knowledge gap through a detailed study on the low frequency noise properties of compact, highly resistive superconducting granular aluminum microwave resonators.³⁰ We observe pronounced fluctuations of the resonance frequency at temperatures of 10–200 mK, which intensify in samples with a higher normal-state resistance. In contrast to conventional aluminum resonators, the $1/f$ noise spectrum of granular aluminum is substantially higher and masked by random telegraphic signal (RTS) like fluctuations. While the amplitude I of the RTS is independent of the measurement power and temperature, the RTS switching time τ_0 abruptly decreases above 200 mK.

The microwave resonators (A1–C3, see [Table I](#)) have been fabricated from three 22–30 nm thick granular aluminum films with different sheet resistances [see [Fig. 1\(a\)](#) for a schematic of its microstructure]. The films were prepared on sapphire substrates by reactive

TABLE I. Characteristics of the measured samples. All resonators have a width of $2\ \mu\text{m}$ but vary in their length l . The average resonance frequency f_0 and resonator linewidth κ are extracted from a fit to the resonance.³¹ R_n is the normal state sheet resistance of the films.

Resonator	f_0 (GHz)	R_n (k Ω)	l (μm)	κ (MHz)
A1	10.565	0.6	406	2.33
B1	5.494	1.4	505	1.84
B2	6.154	1.5	440	2.23
B3	6.793	1.5	390	2.61
C1	4.069	4.0	406	0.61
C2	4.663	4.3	337	0.82
C3	5.780	3.8	287	1.51

sputter deposition of aluminum in an oxygen atmosphere, using an *in situ* control of the sheet resistance.³³ With resistivities up to $\rho = R_n l \sim 10^4\ \mu\Omega\ \text{cm}$, the films are on the same order of magnitude as values reported for the SIT.^{25,26} From each film, multiple half wavelength microstrip resonators coupled to a common transmission line were structured using an optical resist mask and an anisotropic dry etching process. The samples were installed in microwave tight sample box and mounted to the mixing chamber plate of a dry dilution refrigerator, with experimental temperatures ranging from 10 to 400 mK.

The complex transmission coefficient S_{21} in the vicinity of the resonators was measured using a vector network analyzer (VNA). To record the time-dependent frequency fluctuations, the probe frequency was fixed to the average resonator frequency $f_0 \equiv \bar{f}_r$. If the resonator frequency changes by $\delta f_r = f_r - f_0$, the position of $S_{21}(f_0)$ in

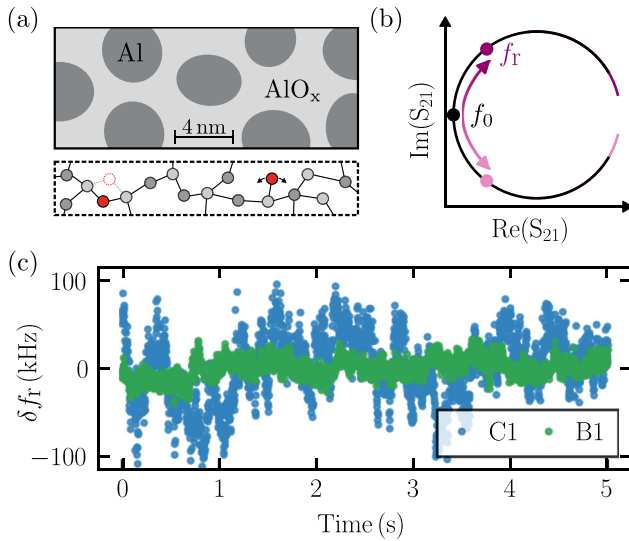


FIG. 1. (a) Top panel: Schematic microstructure of granular aluminum. The grain dimension, location, and the inter-grain AlO_x barrier are subject to disorder.^{15,32} Bottom panel: Two-level defects (red) within the amorphous atomic structure of AlO_x. (b) Sketch of an ideal resonance circle in the complex plane of the transmission signal. A fluctuation of the resonator frequency $\delta f_r = f_r - f_0$ corresponds to a rotation of the circle. This change is monitored by continuously measuring S_{21} with the probe frequency fixed to f_0 . (c) Raw frequency fluctuations of resonator C1 and B1, recorded at an average photon number $\bar{n} \sim 10^4$.

the complex plane proportionately shifts along the resonance circle [see Fig. 1(b)]. Using knowledge of the pre-measured resonance circle, each newly measured value can then be mapped to a corresponding frequency f_r (see the supplementary material for details). A full dataset contains $\mathcal{O}(10^6)$ of such measurements, taken at a rate $\geq 500/\text{s}$.

Figure 1(c) shows extracts from mapped data obtained in typical noise measurements. Compared to the other samples, the fluctuations of the resonance frequency δf_r are much more pronounced in the resonators with the highest sheet resistances (C1–C3), measuring values up to $\delta f_r/\kappa = 0.1$. Here, κ is the individual resonator linewidth.

Our analysis of the frequency fluctuations focuses on the fractional noise spectra defined as $S_y = S_{\delta f_r}/f_0^2$,³⁴ where the power spectral density $S_{\delta f_r}$ (in units of Hz²/Hz) is calculated from the datasets using Welch’s method.³⁵ Figure 2 shows the noise spectrum of resonator C1 compared to the spectrum of a pure aluminum resonator ($R_n \sim 0.3\ \Omega$) measured under identical conditions at $T = 10\ \text{mK}$. For frequencies above 10 Hz, both spectra follow a $1/f$ trend. All granular aluminum samples show, however, orders of magnitude higher noise amplitudes. Additionally, in the region between 0.1 and 10 Hz, the spectrum noticeably deviates from the $1/f$ trend. The spectral shape of these low frequency excess fluctuations indicates an RTS, i.e., the resonator switches between frequency-distinct states. Due to the high $1/f$ noise level, we cannot distinguish experimentally whether random switching occurs between two or more states (Fig. 1).

Similar to previous works,^{36–39} we model their contribution to the spectrum by a Lorentzian centered at zero frequency. This corresponds to a randomly excited process that exponentially decays on a characteristic timescale τ_0 . Including a white noise floor, the full fractional noise spectrum can then be described by the following expression:

$$S_y = \frac{4I^2\tau_0}{1 + (2\pi f\tau_0)^2} + \frac{h_{-1}}{f} + h_0, \quad (1)$$

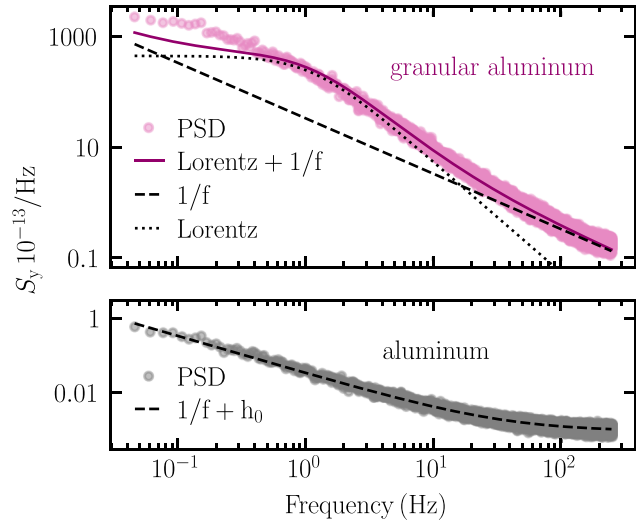


FIG. 2. Low temperature ($T = 10\ \text{mK}$) fractional noise spectra of granular aluminum resonators (here: C1) show a $1/f$ dependency (dashed line), masked by RTS excess noise below 10 Hz (dotted line). Solid line is a fit to Eq. (1). Pure aluminum films measured identically show no sign of RTS noise and orders of magnitude lower $1/f$ noise levels.

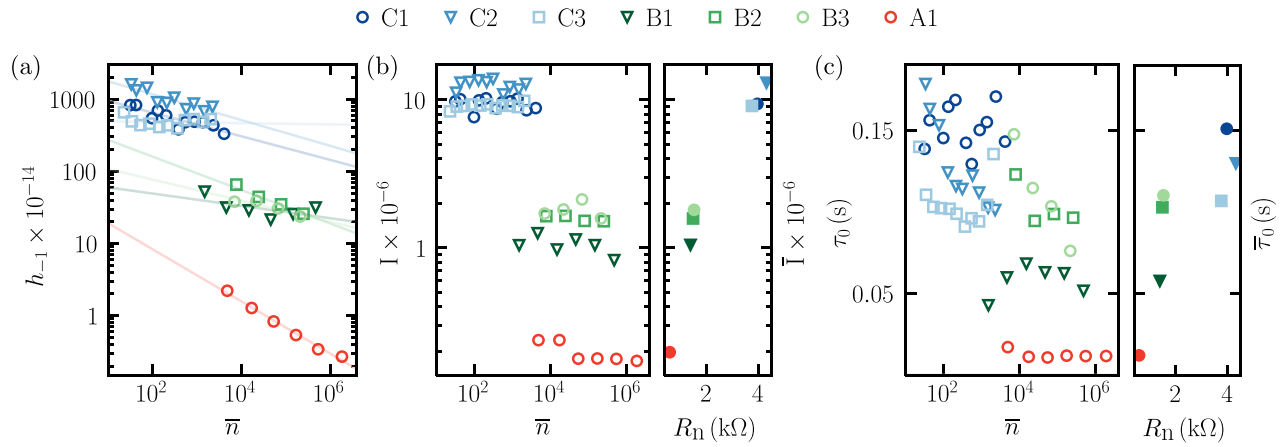


FIG. 3. Power ($\bar{n} \propto P_{MW}$) dependence of the noise parameter. (a) The amplitude h_{-1} of the $1/f$ noise shows a strong dependency on the number of photons in the resonator \bar{n} . Solids lines are a fit to $1/\bar{n}^\beta$. The amplitude I (b) and lifetime τ_0 (c) of the RTS fluctuations are not affected by \bar{n} but shows a noticeable dependency on the film resistance R_n (right panel, respectively).

with the amplitude of the RTS I , the $1/f$ noise h_{-1} and the white noise h_0 , respectively. The following discussion is based on a least squares fit of Eq. (1) to all measured noise spectra.

Figure 3 shows the dependence of the fitting parameters on the average number of photons $\bar{n} = 2P_{VNA}\kappa_c/(\hbar\omega_r^3\kappa^2)$ oscillating in the resonator,⁴⁰ which is controlled by the applied VNA power P_{VNA} . The amplitude of the $1/f$ noise h_{-1} shows a power law dependency, where a comparison to $h_{-1} \propto 1/\bar{n}^\beta$ yields $\beta = 0.36$ (A1), 0.15 ± 0.06 (B1–B3), and 0.12 ± 0.07 (C1–C3), illustrated in Fig. 3(a). However, no clear dependency on \bar{n} can be observed for the parameters of the RTS, despite photon numbers spanning over several orders of magnitude. Note that applied VNA power above $\bar{n} \gg 10^4$ leads to strong non-linear resonance bifurcations^{41,42} in samples C1–C3 and is, therefore, not taken into account. The missing data points of samples A1 and B1–B3 at low photon numbers are due to an obscured (small) RTS signal at an increased $1/f$ amplitude ($h_{-1}/1 \text{ Hz} \geq 4I^2\tau_0$). However, for $\bar{n} \sim 10^4$, the data points overlap and one can, therefore, compare the average values of the RTS amplitude \bar{I} and lifetime $\bar{\tau}_0$ between resonators [Figs. 3(b) and 3(c), right panel]. The comparison indicates a dependency on R_n , which agrees with the initial observations [Fig. 1(c)] that δf_r is most pronounced in resonators made from the most restive film C.

Following the power scans, the dependence of the RTS characteristics on the sample temperature was investigated in the range from 10 to 400 mK. As shown in Fig. 4(a), the RTS lifetime τ_0 decreases rapidly above a threshold temperature of ~ 200 mK in all measured samples. This drop is approximately exponential, as indicated by the black line. The amplitude of the excess fluctuations I , however, remains approximately constant over the whole temperature range [Fig. 4(b)]. Note that $I \propto \delta R_{TS} \times \delta f_r/\delta R_{TS}$, with δR_{TS} the amplitude of the RTS process and $\delta f_r/\delta R_{TS}$ proportional to the coupling between the RTS fluctuators and the resonator.⁴³ Both quantities may have an opposite temperature dependency which cancel out for the overall contribution to I .

The observed $1/f$ scaling of the frequency noise is a well-known phenomenon in thin films that has been studied in widely different systems, revealing a variety of physical sources.⁴⁴ In superconducting

microwave resonators, it is proposed to originate from electric dipole coupling to atomic defects behaving as two-level-systems (TLS), e.g., accumulating in the surface oxide^{45,46} [see Fig. 1(a)].

Within the generalized tunneling model, these TLS are believed to interact with surrounding defects having interlevel transition

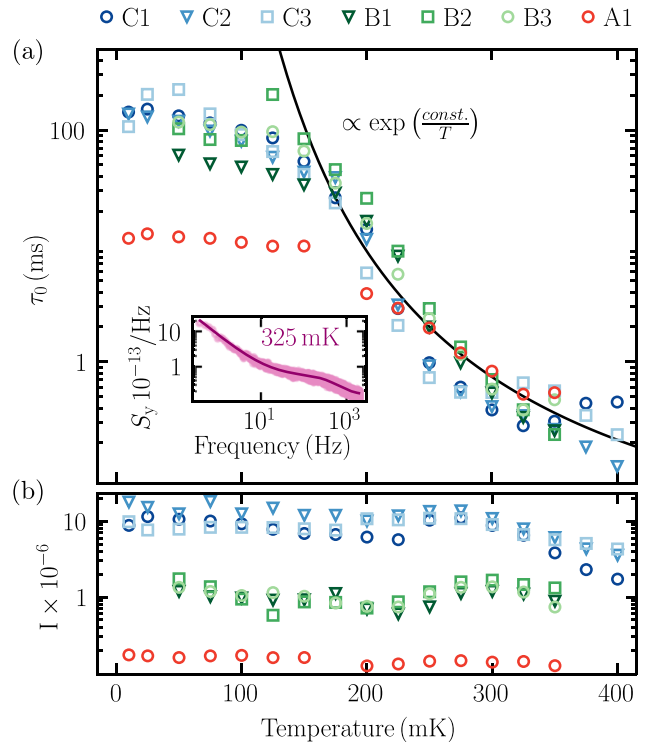


FIG. 4. Temperature dependence of the RTS parameters. While the RTS lifetime τ_0 decreases exponentially (solid line, not a fit) above 200 mK (a), the amplitude I is almost independent of the temperature (b). The inset shows the power spectral density of resonator C1 measured at 325 mK.

frequencies below $k_B T$ and are, therefore, subjected to thermal fluctuations.^{34,47} The superposition of noise from multiple fluctuators results in $1/f$ noise whose amplitude h_{-1} scales with $\beta = 0.5$ at high photon numbers and $\beta \rightarrow 0$ as the photon number decreases,⁴⁸ which qualitatively agrees with our findings. In addition, h_{-1} clearly depends on the sample sheet resistance, which is expected if the number of TLS increases with the thickness of the inter-grain oxide barrier. This complements the observed prevalence of strongly coupled TLS, which we discuss in a separate publication.⁴⁹

In the light of this interpretation, it seems natural to also attribute the RTS noise component to TLS. Indeed, it has been shown in “transmon” type superconducting qubits^{37,38} as well as superconducting resonators³⁹ that a near-resonant TLS can produce a dominant Lorentzian noise spectrum. However, for TLS processes, a reduction of the amplitude I with \bar{n} similar to $h_{-1}(\bar{n})$ would be expected for the resonator-TLS system,³⁹ which we do not observe. Furthermore, due to the random nature of these defects, it is statistically unlikely to find TLS properties only varying between films, but not resonators.

Noise measurements in narrow aluminum resonators showed that quasiparticle generation and recombination noise (g-r noise)⁵⁰ can also produce a Lorentzian noise spectrum.^{36,43} The τ_0 values measured here are comparable to quasiparticle lifetimes previously observed in granular aluminum.⁵¹ For quasiparticles, the exponential decrease in the lifetime depicted in Fig. 4(a) would be expected naturally, as their number N_{qp} increases with temperature and it becomes more likely to find a pairing partner. Since the responsivity of the resonator to quasiparticles $\delta f_i / \delta \text{RTS}$ is likely temperature independent^{52,53} and $\delta \text{RTS} \propto N_{qp}$, the noise amplitude I should instead increase with temperature. The data presented in Fig. 4(b) contradict this assumption, where I rather decreases with increasing temperature. In addition, we do not observe a broadening of the resonance (increase in κ) accompanying the frequency fluctuations, which would be expected for a quasiparticle related origin (see the supplementary material for details).

The strong dependence of the RTS amplitude on the sheet resistance suggests that the origin of the RTS lies in the granular structure of the film, i.e., the interplay between the Josephson coupling and the Coulomb repulsion. While more exotic TLS and quasiparticle processes have been found in highly disordered samples approaching the SIT,^{29,51,54–56} they are also subjected to the concerns brought forward above. A scenario that would, however, be possible is g-r noise due to trapped charges, e.g., on weakly coupled grains¹³ or within the inter-grain oxide barriers.

Another mechanism that becomes relevant in the studied regime are collective modes of the superconducting condensate, i.e., fluctuations of the order parameter Ψ .⁵⁷ In particular, it has been shown theoretically that for a strongly disordered superconductor, phase modes acquire a dipole moment and appear below the gap, where they can have experimentally relevant lifetimes.⁵⁸ Evidence of such modes in granular aluminum has been found in THz spectroscopy^{25,59} and STM measurements.²² Calculations based on the bosonic model of the SIT showed that some modes even extend down to zero frequency where they can be thermally excited. This leads to fluctuations also in higher energy modes due to mode–mode interaction.⁶⁰ However, theoretical frameworks describing the behavior of collective modes more precisely are still under development.⁶¹

In conclusion, we have studied the low frequency excess noise in highly disordered granular aluminum resonators. Our findings

demonstrate that microwave resonator circuits are a valuable tool for the investigation of the SIT in disordered superconductors. The spectral analysis of the data suggests fluctuations of an RTS nature. While the amplitude I of the RTS shows no dependence on the measurement power or the sample temperature, the RTS lifetime τ_0 strongly decreases above a temperature of 200 mK. Our data show a correlation of both RTS amplitude I and lifetime τ_0 with the sheet resistance of the film. The measured absolute values and dependencies suggest that neither TLS nor quasiparticles cause the RTS. Instead, processes related to the reduced inter-grain coupling near the SIT seem to be a more likely explanation for the observed behavior.

In comparison with other superconducting resonators, the measured frequency fluctuations are evidently linked with the nature of the granular material. Until a better understanding (and mitigation) of the physical origin of the RTS fluctuations and $1/f$ excess noise is available, highly resistive granular aluminum films close to the SIT are likely to introduce additional noise in superconducting circuits and detectors.

See the supplementary material for an overview of the experimental setup, details on the resonance frequency tracking, and an Allan analysis of the fluctuations data.

The authors thank T. Wolz, M. Spiecker, J. Lisenfeld, M. Feigel'man, and J. Cole for helpful discussions and L. Radtke for technical support. Samples were fabricated in the KIT Nanostructure Service Laboratory (NSL). This work was supported by the German Federal Ministry of Education and Research (GeQCoS and QSolid). The authors acknowledge the partial support from the Landesgraduiertenförderung of the state Baden-Württemberg (M.W.) and the Helmholtz International Research School for Teratronics (J.N.V.).

AUTHOR DECLARATIONS

Conflict of Interest

The authors have no conflicts to disclose.

Author Contributions

Maximilian Kristen: Conceptualization (equal); Data curation (equal); Formal analysis (lead); Investigation (equal); Methodology (equal); Validation (equal); Visualization (lead); Writing – original draft (lead). **Jan Nicolas Voss:** Conceptualization (equal); Data curation (equal); Formal analysis (supporting); Investigation (equal); Methodology (equal); Validation (equal); Writing – review & editing (equal). **Micha Wildermuth:** Conceptualization (equal); Methodology (equal); Validation (equal); Writing – review & editing (equal). **Hannes Rotzinger:** Conceptualization (equal); Funding acquisition (equal); Methodology (equal); Resources (equal); Supervision (equal); Validation (equal); Writing – review & editing (equal). **Alexey V. Ustinov:** Conceptualization (equal); Funding acquisition (equal); Resources (equal); Supervision (equal); Writing – review & editing (equal).

DATA AVAILABILITY

The data that support the findings of this study are available from the corresponding author upon reasonable request.

REFERENCES

- ¹Y. Dubi, Y. Meir, and Y. Avishai, *Nature* **449**, 876 (2007).
- ²B. Sacépé, M. Feigel'man, and T. M. Klapwijk, *Nat. Phys.* **16**, 734 (2020).
- ³A. T. Bollinger, G. Dubuis, J. Yoon, D. Pavuna, J. Misewich, and I. Božović, *Nature* **472**, 458 (2011).
- ⁴D. T. Harris, N. Campbell, R. Uecker, M. Brützmam, D. G. Schlom, A. Levchenko, M. S. Rzchowski, and C.-B. Eom, *Phys. Rev. Mater.* **2**, 041801 (2018).
- ⁵Y. Zhou, J. Guo, S. Cai, J. Zhao, G. Gu, C. Lin, H. Yan, C. Huang, C. Yang, S. Long, Y. Gong, Y. Li, X. Li, Q. Wu, J. Hu, X. Zhou, T. Xiang, and L. Sun, *Nat. Phys.* **18**, 406 (2022).
- ⁶B. Douçot and L. B. Ioffe, *Rep. Prog. Phys.* **75**, 072001 (2012).
- ⁷J. Baselmans, *J. Low Temp. Phys.* **167**, 292 (2012).
- ⁸J. Zmuidzinias, *Annu. Rev. Condens. Matter Phys.* **3**, 169 (2012).
- ⁹I. S. Beloborodov, A. V. Lopatin, V. M. Vinokur, and K. B. Efetov, *Rev. Mod. Phys.* **79**, 469 (2007).
- ¹⁰U. S. Pracht, N. Bachar, L. Benfatto, G. Deutscher, E. Farber, M. Dressel, and M. Scheffler, *Phys. Rev. B* **93**, 100503 (2016).
- ¹¹P. W. Anderson, *Lectures on the Many-Body Problems* (Academic, New York, 1964), Vol. 2.
- ¹²B. Abeles, *Phys. Rev. B* **15**, 2828 (1977).
- ¹³K. B. Efetov, *Sov. Phys. JETP* **51**, 1015 (1980), available at http://jetp.ras.ru/cgi-bin/dn/e_051_05_1015.pdf.
- ¹⁴V. Humbert, M. Ortuño, A. M. Somoza, L. Bergé, L. Dumoulin, and C. A. Marrache-Kikuchi, *Nat. Commun.* **12**(1), 6733 (2021).
- ¹⁵J. N. Voss, Y. Schön, M. Wildermuth, D. Dorer, J. H. Cole, H. Rotzinger, and A. V. Ustinov, *ACS Nano* **15**, 4108 (2021).
- ¹⁶S. Chakravarty, S. Kivelson, G. T. Zimanyi, and B. I. Halperin, *Phys. Rev. B* **35**, 7256 (1987).
- ¹⁷H. M. Jaeger, D. B. Haviland, B. G. Orr, and A. M. Goldman, *Phys. Rev. B* **40**, 182 (1989).
- ¹⁸K. Bouadim, Y. L. Loh, M. Randeria, and N. Trivedi, *Nat. Phys.* **7**, 884 (2011).
- ¹⁹B. Sacépé, T. Dubouchet, C. Chapelier, M. Sanquer, M. Ovidia, D. Shahar, M. Feigel'man, and L. Ioffe, *Nat. Phys.* **7**, 239 (2011).
- ²⁰D. Sherman, U. S. Pracht, B. Gorshunov, S. Poran, J. Jesudasan, M. Chand, P. Raychaudhuri, M. Swanson, N. Trivedi, A. Auerbach, M. Scheffler, A. Frydman, and M. Dressel, *Nat. Phys.* **11**, 188 (2015).
- ²¹T. Dubouchet, B. Sacépé, J. Seidemann, D. Shahar, M. Sanquer, and C. Chapelier, *Nat. Phys.* **15**, 233 (2019).
- ²²F. Yang, T. Gozinski, T. Storbeck, L. Grünhaupt, I. M. Pop, and W. Wulfhchel, *Phys. Rev. B* **102**, 104502 (2020).
- ²³U. S. Pracht, M. Scheffler, M. Dressel, D. F. Kalok, C. Strunk, and T. I. Baturina, *Phys. Rev. B* **86**, 184503 (2012).
- ²⁴D. Sherman, B. Gorshunov, S. Poran, N. Trivedi, E. Farber, M. Dressel, and A. Frydman, *Phys. Rev. B* **89**, 035149 (2014).
- ²⁵F. Levy-Bertrand, T. Klein, T. Grenet, O. Dupré, A. Benoît, A. Bideaud, O. Bourrion, M. Calvo, A. Catalano, A. Gomez, J. Goupy, L. Grünhaupt, U. v Luepke, N. Maleeva, F. Valenti, I. M. Pop, and A. Monfardini, *Phys. Rev. B* **99**, 094506 (2019).
- ²⁶R. C. Dynes, J. P. Garno, G. B. Hertel, and T. P. Orlando, *Phys. Rev. Lett.* **53**, 2437 (1984).
- ²⁷H. M. Jaeger, D. B. Haviland, A. M. Goldman, and B. G. Orr, *Phys. Rev. B* **34**, 4920 (1986).
- ²⁸Z. Han, A. Allain, H. Arjmandi-Tash, K. Tikhonov, M. Feigel'man, B. Sacépé, and V. Bouchiat, *Nat. Phys.* **10**, 380 (2014).
- ²⁹A. Roy, Y. Wu, R. Berkovits, and A. Frydman, *Phys. Rev. Lett.* **125**, 147002 (2020).
- ³⁰H. Rotzinger, S. T. Skacel, M. Pfirrmann, J. N. Voss, J. Münzberg, S. Probst, P. Bushev, M. P. Weides, A. V. Ustinov, and J. E. Mooij, *Supercond. Sci. Technol.* **30**, 025002 (2017).
- ³¹S. Probst, F. B. Song, P. A. Bushev, A. V. Ustinov, and M. Weides, *Rev. Sci. Instrum.* **86**, 024706 (2015).
- ³²T. C. Bartolo, J. S. Smith, Y. Schön, J. N. Voss, M. J. Cyster, A. V. Ustinov, H. Rotzinger, and J. H. Cole, *New J. Phys.* **24**, 073008 (2022).
- ³³M. Wildermuth, L. Powalla, J. N. Voss, Y. Schön, A. Schneider, M. V. Fistul, H. Rotzinger, and A. V. Ustinov, *Appl. Phys. Lett.* **120**, 112601 (2022).
- ³⁴J. Burnett, L. Faoro, I. Wisby, V. L. Gurtovoi, A. V. Chernykh, G. M. Mikhailov, V. A. Tulin, R. Shaikhaidarov, V. Antonov, P. J. Meeson, A. Y. Tzalenchuk, and T. Lindström, *Nat. Commun.* **5**, 4119 (2014).
- ³⁵P. Welch, *IEEE trans. Audio Electroacoust.* **15**, 70 (1967).
- ³⁶P. J. de Visser, J. J. A. Baselmans, P. Diener, S. J. C. Yates, A. Endo, and T. M. Klapwijk, *Phys. Rev. Lett.* **106**, 167004 (2011).
- ³⁷S. Schlör, J. Lisenfeld, C. Müller, A. Bilmes, A. Schneider, D. P. Pappas, A. V. Ustinov, and M. Weides, *Phys. Rev. Lett.* **123**, 190502 (2019).
- ³⁸J. J. Burnett, A. Bengtsson, M. Scigliuzzo, D. Niepce, M. Kudra, P. Delsing, and J. Bylander, *npj Quantum Inf.* **5**, 54 (2019).
- ³⁹D. Niepce, J. J. Burnett, M. Kudra, J. H. Cole, and J. Bylander, *Sci. Adv.* **7**, 462 (2021).
- ⁴⁰A. Schneider, Ph.D. thesis, Karlsruhe Institute of Technology, 2020.
- ⁴¹L. J. Swenson, P. K. Day, B. H. Eom, H. G. Leduc, N. Llombart, C. M. McKenney, O. Noroozian, and J. Zmuidzinias, *J. Appl. Phys.* **113**, 104501 (2013).
- ⁴²Q. He, P. OuYang, M. Dai, H. Guan, J. Hu, S. He, Y. Wang, and L. F. Wei, *AIP Adv.* **11**, 065204 (2021).
- ⁴³P. J. de Visser, J. J. A. Baselmans, S. J. C. Yates, P. Diener, A. Endo, and T. M. Klapwijk, *Appl. Phys. Lett.* **100**, 162601 (2012).
- ⁴⁴S. Kogan, *Electronic Noise and Fluctuations in Solids* (Cambridge University Press, Cambridge, 1996).
- ⁴⁵E. Paladino, Y. Galperin, G. Falci, and B. Altshuler, *Rev. Mod. Phys.* **86**, 361 (2014).
- ⁴⁶C. Müller, J. H. Cole, J. Lisenfeld, C. E. Professor, and S. Washburn, *Rep. Prog. Phys.* **82**, 124501 (2019).
- ⁴⁷L. Faoro and L. B. Ioffe, *Phys. Rev. Lett.* **109**, 157005 (2012).
- ⁴⁸L. Faoro and L. B. Ioffe, *Phys. Rev. B* **91**, 014201 (2015).
- ⁴⁹M. Kristen, J. N. Voss, M. Wildermuth, J. Lisenfeld, H. Rotzinger, and A. V. Ustinov, "Observation of giant two-level-systems in a granular superconductor" (unpublished).
- ⁵⁰C. M. Wilson and D. E. Prober, *Phys. Rev. B* **69**, 094524 (2004).
- ⁵¹L. Grünhaupt, N. Maleeva, S. T. Skacel, M. Calvo, F. Levy-Bertrand, A. V. Ustinov, H. Rotzinger, A. Monfardini, G. Catelani, and I. M. Pop, *Phys. Rev. Lett.* **121**, 117001 (2018).
- ⁵²J. Baselmans, S. J. C. Yates, R. Barends, Y. J. Y. Lankwarden, J. R. Gao, H. Hoevers, and T. M. Klapwijk, *J. Low Temp. Phys.* **151**, 524 (2008).
- ⁵³J. Gao, J. Zmuidzinias, A. Vayonakis, P. Day, B. Mazin, and H. Leduc, *J. Low Temp. Phys.* **151**, 557 (2008).
- ⁵⁴S. E. de Graaf, L. Faoro, L. B. Ioffe, S. Mahashabde, J. J. Burnett, T. Lindström, S. E. Kubatkin, A. V. Danilov, and A. Y. Tzalenchuk, *Sci. Adv.* **6**, eabc5055 (2020).
- ⁵⁵C. Barone, H. Rotzinger, C. Mauro, D. Dorer, J. Münzberg, A. V. Ustinov, and S. Pagano, *Sci. Rep.* **8**, 13892 (2018).
- ⁵⁶C. Barone, H. Rotzinger, J. N. Voss, C. Mauro, Y. Schön, A. V. Ustinov, and S. Pagano, *Nanomaterials* **10**, 524 (2020).
- ⁵⁷P. Raychaudhuri and S. Dutta, *J. Phys.: Condens. Matter* **34**, 083001 (2022).
- ⁵⁸T. Cea, D. Bucheli, G. Seibold, L. Benfatto, J. Lorenzana, and C. Castellani, *Phys. Rev. B* **89**, 174506 (2014).
- ⁵⁹U. S. Pracht, T. Cea, N. Bachar, G. Deutscher, E. Farber, M. Dressel, M. Scheffler, C. Castellani, A. M. García-García, and L. Benfatto, *Phys. Rev. B* **96**, 094514 (2017).
- ⁶⁰M. Feigel'man and L. Ioffe, *Phys. Rev. Lett.* **120**, 037004 (2018).
- ⁶¹A. V. Khvalyuk and M. V. Feigel'man, *Phys. Rev. B* **104**, 224505 (2021).